
^{68}Ga -Labeled Bombesin Studies in Patients with Gastrointestinal Stromal Tumors: Comparison with ^{18}F -FDG

Antonia Dimitrakopoulou-Strauss¹, Peter Hohenberger², Uwe Haberkorn^{1,3}, Helmut R. Mäcke⁴, Michael Eisenhut⁵, and Ludwig G. Strauss¹

¹Medical PET Group—Biological Imaging, Clinical Cooperation Unit Nuclear Medicine, German Cancer Research Center, Heidelberg, Germany; ²Division of Surgical Oncology and Thoracic Surgery, Surgical Clinic, Klinikum Mannheim, University of Heidelberg, Heidelberg, Germany; ³Department of Nuclear Medicine, University of Heidelberg, Heidelberg, Germany; ⁴Division of Radiological Chemistry, Department of Radiology, University Hospital Basel, Basel, Switzerland; and ⁵Department of Radiopharmaceutical Chemistry, German Cancer Research Center, Heidelberg, Germany

Dynamic PET studies with a ^{68}Ga -bombesin analog, DOTA-PEG₂-[D-Tyr⁶, β-Ala¹¹, Thi¹³, Nle¹⁴] BN(6-14) amide (^{68}Ga -BZH₃; DOTA is 1,4,7,10-tetraazacyclododecane-*N,N',N'',N'''*-tetraacetic acid, and PEG is ethylene glycol [2-aminoethyl-carboxymethyl ether]), were performed on patients with gastrointestinal stromal tumors (GIST) to investigate the impact of complementary receptor scintigraphy on diagnosis and the potential of a radionuclide treatment. Furthermore, dynamic ^{18}F -FDG studies were performed on the same patients. **Methods:** This study comprised 17 patients with GIST. All patients were scheduled for therapy with imatinib because of unresectable primary or recurrent GIST or because of metastatic disease. Dynamic PET scans using ^{68}Ga -BZH₃ and ^{18}F -FDG were obtained on 2 consecutive days. Multivariate analysis was used to evaluate the kinetic data. Standardized uptake values (SUVs) were calculated, and a compartmental model (2-tissue) and noncompartmental model were used for data evaluation of both tracers. **Results:** Fourteen of 17 patients (25/30 lesions) were positive for uptake on ^{18}F -FDG imaging, whereas ^{68}Ga -BZH₃ demonstrated an enhanced accumulation in 7 of 17 patients (8/30 lesions). Thirteen lesions were confirmed by histologic examination, and the remaining 17 were confirmed by follow-up. One recurrent tumor in the stomach could not be delineated on ^{18}F -FDG imaging but showed enhanced ^{68}Ga -BZH₃ uptake. The median SUV for ^{68}Ga -BZH₃ was 3.3, in comparison with 7.9 for ^{18}F -FDG. Best-subset analysis demonstrated that the global SUV (55–60 min after injection) for ^{18}F -FDG was primarily dependent on k₃, followed by k₁. Multivariate analysis did not show a significant correlation between the kinetic parameters (k₁–k₄, fractional blood volume, and SUV) for ^{18}F -FDG and bombesin. **Conclusion:** ^{68}Ga -BZH₃ may be helpful for diagnostic reasons in a subgroup of patients with GIST, as in the case of negative ^{18}F -FDG findings and suspicion of viable tumor tissue.

The meaning of the enhanced ^{68}Ga -BZH₃ uptake is open at the moment.

Key Words: ^{68}Ga -bombesin; ^{18}F -FDG; GIST; PET; kinetic modeling

J Nucl Med 2007; 48:1245–1250
DOI: 10.2967/jnumed.106.038091

Gastrointestinal stromal tumors (GIST) are tumors that occur in the wall of the bowel and are thought to be derived from the cells of Cajal, which drive peristalsis in the intestine. Most GIST show a gain-of-function mutation in the cKIT proto-oncogene resulting in ligand-independent activation of the cKIT receptor tyrosine kinase (*J*). PET with ^{18}F -FDG is frequently used for oncologic applications to assess tissue viability. Especially in patients with GIST, ^{18}F -FDG is being used for staging and therapy monitoring. Not all patients respond to imatinib mesylate, and many of those who initially respond may later become resistant. Therefore, new therapeutic approaches are needed. One idea is to study the expression of different receptors to guide therapy in that direction. It has recently been shown that somatostatin receptors can be quite well imaged using a new radiolabeled compound, ^{68}Ga -DOTA-D-Phe¹-Tyr³-octreotide (DOTATOC). In patients with neuroendocrine tumors, DOTATOC has successfully been used both for diagnostic purposes, labeled with ^{68}Ga , and for therapy, labeled with ^{90}Y (2). Reubi et al. reported in a recent paper that GIST expressed bombesin subtype 2 receptors, better known as gastrin-releasing peptide receptors, using in vitro receptor autoradiography (3). The authors reported that not only primary GIST but also metastases and even tumor samples from patients who did not respond to imatinib were receptor-positive. On the basis of these data, in patients with GIST we used for the first time ^{68}Ga -bombesin, in terms of a pan-bombesin analog, the peptide DOTA-PEG₂-[D-Tyr⁶,

Received Nov. 12, 2006; revision accepted Apr. 23, 2007.
For correspondence or reprints contact: Antonia Dimitrakopoulou-Strauss, MD, Medical PET Group—Biological Imaging (E0601), Clinical Cooperation Unit Nuclear Medicine, German Cancer Research Center, Im Neuenheimer Feld 280, D-69120 Heidelberg, Germany.
E-mail: ads@ads-lgs.de or a.dimitrakopoulou-strauss@dkfz.de
COPYRIGHT © 2007 by the Society of Nuclear Medicine, Inc.

β -Ala¹¹,Thi¹³,Nle¹⁴] BN(6-14) amide (BZH₃; DOTA is 1,4,7,10-tetraazacyclododecane-*N,N',N'',N'''*-tetraacetic acid, and PEG is ethylene glycol [2-aminoethyl-carboxymethyl ether]).

Because of the increased spatial resolution of PET and its ability to quantify biodistribution, the pan-bombesin analog BZH₃ was labeled with the positron emitter ⁶⁸Ga, which has a half-life of 68.3 min for the positron emission (4). BZH₃ binds to at least 3 receptor subtypes: bombesin receptor subtypes 1 (also known as neuromedin B), 2, and 3. The aim of this study was to investigate the impact of complementary receptor scintigraphy on diagnosis and the potential of a radionuclide treatment. Furthermore, bombesin kinetics were compared with ¹⁸F-FDG kinetics. We compared the bombesin kinetic data derived from a 60-min full dynamic acquisition with those obtained from the dynamic ¹⁸F-FDG data. For quantitative analysis of both tracers, a 2-tissue-compartment model and a noncompartment model based on the fractal dimension were used. In particular, we evaluated different kinetic parameters such as k_1 – k_4 and V_B , which reflects the fraction of blood within the evaluated volume, and compared them with global tracer uptake (SUV) to find which parameter has the greatest impact.

MATERIALS AND METHODS

⁶⁸Ga for PET was obtained from a ⁶⁸Ge/⁶⁸Ga generator, which consists of a column containing a phenolic ion exchanger (manufactured in-house) loaded with ⁶⁸Ge and coupled in series with a small-sized anion-exchanger column (AG 1 × 8 Cl⁻ ion-exchange resin, 200–400 mesh; Bio-Rad) to concentrate ⁶⁸Ga during elution. This generator provides ⁶⁸Ga with an average yield of 60% for more than 1.5 y. ⁶⁸Ga-BZH₃ was prepared according to the method described by Schuhmacher et al. (4).

For ¹⁸F-FDG studies, all patients fasted for at least 4 h before undergoing PET. Blood glucose levels were measured immediately before PET began and were within normal levels (<130 mg/dL). ¹⁸F-FDG was prepared according to the method described by Toorongian et al. (5).

The study included 17 patients with histologically proven GIST. Two of the patients had primary GIST without previous treatment and were scheduled for preoperative imatinib therapy because of unresectable tumors. The remaining 15 patients were previously treated with surgery and were scheduled for imatinib therapy because of suggestive metastatic lesions on CT or MRI. Five of these patients received imatinib before undergoing PET. All 17 patients were scheduled for imatinib therapy and underwent an ¹⁸F-FDG PET study for staging and a bombesin PET study for assessment of bombesin receptor expression. Dynamic PET studies were performed for 60 min after the intravenous application of 300–370 MBq of ¹⁸F-FDG and 150–210 MBq of ⁶⁸Ga-BZH₃ (3 nmol) using a 28-frame protocol (10 frames of 30 s, 5 frames of 60 s, 5 frames of 120 s, and 8 frames of 300 s) on 2 consecutive days. A dedicated PET system (ECAT EXACT HR+; Siemens) with an axial field of view of 15.3 cm, operated with septa extended (2-dimensional mode), was used for patient studies. The system allows the simultaneous acquisition of 63 transaxial slices with a theoretic slice thickness of 2.4 mm. Before application of the radionuclide, transmission scans for a total of 10 min were obtained for attenuation correction of the acquired emission tomographic images. All PET images were corrected for

attenuation, and an image matrix of 256 × 256 pixels was used for iterative image reconstruction. Conversion of reconstructed images to SUV images was based on the following formula (6): standardized uptake value (SUV) = tissue concentration (Bq/g)/(injected dose [Bq]/body weight [g]). The SUV 55–60 min after injection was used for the analysis of both tracers.

Dynamic PET data were evaluated using the software package PMOD (provided courtesy of PMOD Technologies Ltd.) (7,8). Areas with enhanced tracer uptake on transaxial, coronal, and sagittal images were evaluated visually. Time–activity curves were created using volumes of interest. A volume of interest consists of several regions of interest over the target area. Irregular regions of interest were drawn manually. To compensate for possible patient motion during the acquisition, the original regions of interest were visually repositioned but not redrawn. A detailed quantitative evaluation of tracer kinetics requires the use of compartmental modeling. A 2-tissue-compartment model was used to evaluate the dynamic studies. This methodology is standard, particularly for the quantification of dynamic ¹⁸F-FDG studies (9,10).

One problem in patient studies is accurate measurement of the input function, which theoretically requires arterial blood sampling. However, the input function can be retrieved from the image data with good accuracy (11). For the input function, the mean value of the volume-of-interest data obtained from a large artery, such as the descending aorta, was used. The constants k_1 – k_4 were calculated using a 2-compartment model implemented in the PMOD software taking into account V_B in a volume of interest as an additional variable. Details about the applied compartmental model have been described by Burger and Buck (7). The model parameters were accepted when k_1 – k_4 was less than 1 and V_B exceeded 0. The unit for the rate constants k_1 – k_4 was 1/min.

Concerning the ⁶⁸Ga-BZH₃ kinetics, again the 2-tissue-compartment model was applied to the data. In the case of ⁶⁸Ga-BZH₃, k_1 is associated with receptor binding, k_2 with displacement from the receptor, k_3 with cellular internalization, and k_4 with externalization. For ¹⁸F-FDG, k_1 is associated with influx of the tracer, k_2 with efflux, k_3 with phosphorylation, and k_4 with dephosphorylation. V_B , which is associated with the volume of blood exchanging with tissue, was calculated as a separate parameter.

Besides the compartmental analysis, a noncompartmental model based on the fractal dimension was used. The fractal dimension is a parameter of heterogeneity and was calculated for the time–activity data of each individual volume of interest. The values for fractal dimension vary from 0 to 2, showing the deterministic or chaotic distribution of tracer activity. We used a subdivision of 7 × 7 and a maximal SUV of 20 for the calculation of fractal dimension (12).

The data were statistically evaluated using JMP IN software (version 5.1; SAS Institute GmbH) on a notebook computer (MacBook Pro, 2.16 GHz, 2 GB of random-access memory; Apple) running with the Mac OS X operating system (Apple). The statistical evaluation used descriptive statistics, box plots, and linear regression analysis. The parameters for measuring linear fit were determined by the least-squares method.

Each patient gave written informed consent to participate in the study and to have their medical records released. The study was performed with the approval of the institutional review board.

RESULTS

The evaluation comprised 17 patients with 30 lesions, including 2 primary lesions (stomach and rectum), 3 recurrent

lesions (stomach), and 25 metastatic lesions (12 liver metastases, 10 gut lesions, 2 pelvic lesions, and 1 soft-tissue metastasis in the upper leg). All study patients were scheduled for therapy with imatinib because of unresectable primary or recurrent GIST or because of metastatic disease. Of the 30 evaluated lesions, 13 were confirmed by histologic evaluation and 17 by clinical follow-up. Fourteen of 17 patients (25/30 lesions) showed increased ^{18}F -FDG uptake in the primary or recurrent tumor or in the metastases. Two hypermetabolic areas were falsely classified as tumors on the basis of the ^{18}F -FDG findings. These 2 findings were in the gastroesophageal junction (average SUV, 2.8) and in the colon ascendens (average SUV, 3.5). The lack of correlative pathologic findings on CT and MRI and on clinical follow-up confirmed that these ^{18}F -FDG findings were not due to malignancy. Four lesions in 2 patients who received imatinib therapy were true-negative on the basis of clinical follow-up data. A lesion in a patient with recurrent, histologically confirmed GIST of the stomach could not be delineated on the ^{18}F -FDG scan (false-negative). Comparison with the histologic data revealed a low proliferative activity, with a Ki-67 of less than 10%, in this patient. However, this recurrent tumor showed enhanced ^{68}Ga -BZH₃ uptake (Fig. 1).

We noted physiologically uniform enhanced ^{68}Ga -BZH₃ uptake in the entire pancreas of all patients. ^{68}Ga -BZH₃ uptake in the evaluated tumor lesions was generally lower than ^{18}F -FDG uptake, and 8 of 30 evaluated lesions (7/17 patients) could be delineated through the enhanced bombesin uptake. We found no difference in ^{68}Ga -bombesin uptake with respect to imatinib pretreatment. Two of 5 patients who received imatinib before PET demonstrated enhanced ^{68}Ga -BZH₃ uptake. Figure 2 shows an example of a patient with GIST of the stomach and a suggestive metastatic lesion medial to the spleen (Fig. 2A). The ^{18}F -FDG images clearly showed enhanced ^{18}F -FDG uptake in this area (Fig. 2B). The bombesin images showed diffuse enhanced uptake ventral to the spleen (Fig. 2C). Figure 3 demonstrates another patient with 2 suggestive lesions on CT, one in the stomach and a smaller one in the right liver lobe. Whereas both lesions could be delineated clearly on the ^{18}F -FDG images because of hypermetabolism, the bombesin images revealed enhanced uptake of the labeled peptide primarily in the smaller lesion in the liver. Histologic examination revealed recurrent GIST of the stomach and a liver metastasis.

The 56- to 60-min SUV for ^{68}Ga -BZH₃ was highly variable, with a range of 0.5–9.3 (median, 3.3). The 56- to 60-min SUV for ^{18}F -FDG was higher, with a range of 2.4–17.0 (median, 7.9). k_1 , k_2 , and in particular k_3 for ^{68}Ga -BZH₃ were lower than the corresponding values for ^{18}F -FDG, whereas V_B was higher for bombesin (Table 1).

Box plots of ^{18}F -FDG and ^{68}Ga -BZH₃ uptake (56- to 60-min SUV) in tumor tissue are presented in Figure 4A. The transport rate constants k_1 and k_3 and the vascular fraction V_B of both tracers are presented in Figure 4B. The data show higher SUV, k_1 , and k_3 values for ^{18}F -FDG than for bombesin. V_B was higher for bombesin. No significant correlation was found between the kinetic parameters of bombesin and of ^{18}F -FDG for the evaluated lesions.

We used linear regression analysis to determine the effect of each kinetic parameter (k_1 – k_4 and V_B) on global SUV. Analysis of the ^{18}F -FDG data revealed the highest positive F score for k_3 ($F = 8.5$, $P = 0.008$), followed by k_1 ($F = 5.7$, $P = 0.025$). The bombesin data could not be analyzed because of the low number of positive lesions.

DISCUSSION

^{18}F -FDG still has a major impact on the diagnostics and management of patients with GIST (13,14). Although ^{18}F -FDG is the tracer of choice, the aim of this study was to investigate the impact of complementary receptor scintigraphy on diagnosis and the potential for a radionuclide treatment, such as ^{90}Y -DOTATOC treatment of patients with neuroendocrine tumors. Furthermore, the study compared the kinetic data of ^{68}Ga -BZH₃ with those of ^{68}Ga -DOTATOC and ^{18}F -FDG.

Receptor imaging has found a use in nuclear oncology, with somatostatin receptor imaging being widely used in oncologic patients, primarily those with neuroendocrine tumors. We have reported ^{68}Ga -DOTATOC studies on patients with neuroendocrine tumors, meningiomas, and non-small cell lung cancer (2,15). Bombesin analogs labeled with γ - or β -emitting radionuclides have found some limited use for imaging prostate cancer, breast carcinoma, and small cell lung tumors. Gastrin-releasing peptide receptors were found to be predominantly expressed in human prostate cancer (100%), gastrinoma (100%), and breast cancer (70%), whereas concomitant expression of gastrin-releasing peptide

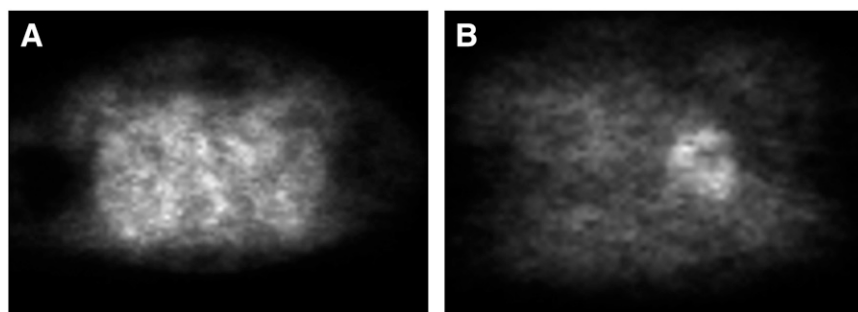


FIGURE 1. Patient with recurrent GIST in stomach. (A) Transaxial ^{18}F -FDG image (SUV image) at level of upper abdomen shows no significantly enhanced ^{18}F -FDG uptake in stomach. (B) Corresponding transaxial bombesin image (SUV image) at level of upper abdomen shows enhanced bombesin uptake in stomach (SUV, 9.3).

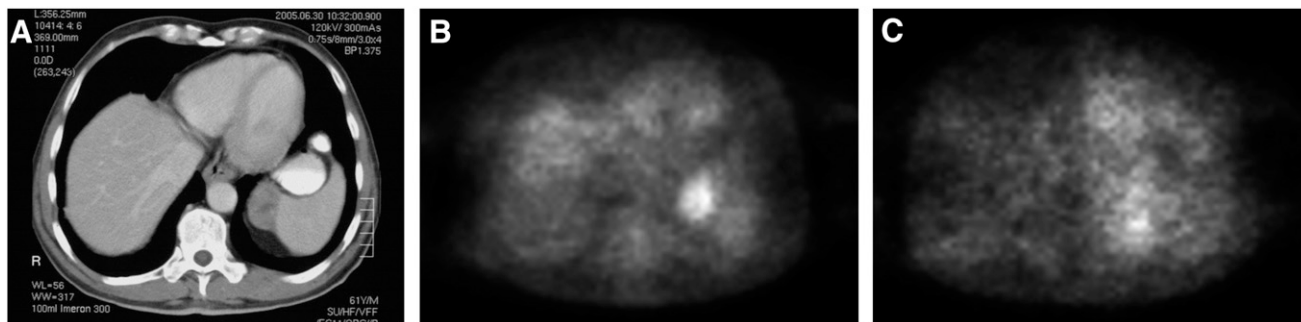


FIGURE 2. (A) CT image of patient with metastatic GIST demonstrates soft-tissue mass medial to spleen. (B) Transaxial ^{18}F -FDG image (SUV image) at level of CT image shows enhanced ^{18}F -FDG uptake (SUV, 3.2) at location of CT finding. (C) Corresponding transaxial bombesin image (SUV image) at level of CT image shows slightly enhanced bombesin uptake (SUV, 2.0) at location of CT finding.

receptors (33%) and bombesin receptor subtype 3 (40%) was found in small cell lung cancer (16). These data are comparable to our currently presented results on GIST patients, only a subgroup of whom demonstrated enhanced ^{68}Ga -BZH₃ uptake. However, because of the lack of immunohistochemical studies in this study, the question is open as to whether enhancement of ^{68}Ga -BZH₃ uptake was due to overexpression of only one bombesin receptor subtype or of all.

We used a pan-bombesin analog, BZH₃, labeled with ^{68}Ga . Experimental results on rats have been reported by Zhang et al. using ^{111}In - and ^{177}Lu -labeled pan-bombesin peptides, BZH₁, and BZH₂. The authors performed biodis-

tribution studies on Lewis rats bearing a rat pancreatic carcinoma cell line, AR4-2J, which is known to express high levels of bombesin receptors (16). Zhang et al. reported a high uptake for both of these radiolabeled peptides in AR4-2J tumors and in organs—such as the pancreas—positive for gastrin-releasing peptide receptor. The high pancreatic uptake is comparable to our results in GIST patients. We noted homogeneously enhanced ^{68}Ga -BZH₃ uptake in the normal pancreatic tissue of all examined patients. Schuhmacher et al. performed biodistribution studies with ^{68}Ga -BZH₃ on rats bearing the same pancreatic tumor cell line, AR4-2J (4). The authors found a high affinity for ^{68}Ga -BZH₃ and rapid internalization. Clearance of ^{68}Ga -BZH₃ from the circulation and from normal tissues negative for gastrin-releasing peptide receptor was fast and resulted in low background activity and high tumor-to-tissue ratios as early as 1 h after injection (4). On the basis of these data, we decided to use a 60-min acquisition protocol for the ^{68}Ga -BZH₃ studies. The quantitative analysis was based on the 2-tissue-compartment model because receptor binding is given by k_1 . Schuhmacher et al. reported a high receptor affinity in cells and a low nonspecific binding of the tracer (<3.5%). Furthermore, they reported a high internalization rate, which is reflected by k_3 , when using the 2-tissue-compartment model. The fraction of internalized ^{68}Ga -BZH₃ activity compared with total cell-associated activity was 85% after 1 h of incubation in AR4-2J cells. This value indicates a primarily enhanced expression of bombesin receptor subtype 1 and bombesin receptor subtype 2.

One important aspect of PET is the possibility of performing noninvasive highly accurate quantitative measurements of tracer concentration in patients. The use of a 2-compartment model is generally an accepted approach to the assessment of ^{18}F -FDG kinetics (10). Concerning bombesin kinetics, k_1 is a parameter that reflects receptor binding, and k_3 is a parameter that reflects internalization of the tracer. Unfortunately, only a few studies have been performed on humans to assess rate constants in malignant tumors, and to our knowledge, no data have been published on the kinetics of ^{68}Ga -BZH₃ in patients. Kinetic data exist

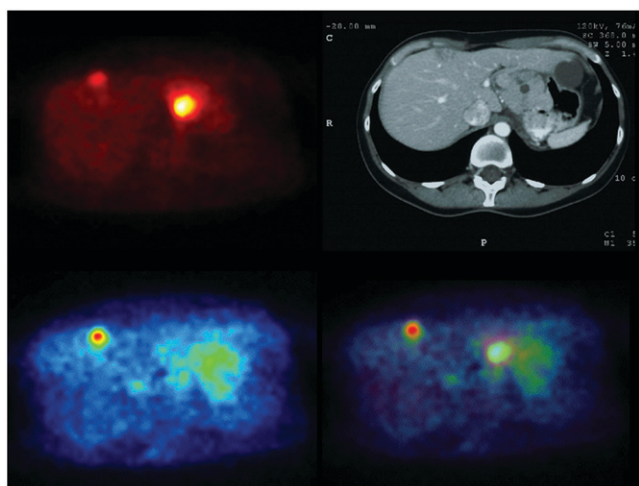


FIGURE 3. (Top left) Transaxial ^{18}F -FDG image (SUV image) at level of liver demonstrates 2 hypermetabolic areas, one in ventral part of right liver lobe (SUV, 5.8) and another in stomach (SUV, 17.1), in patient with metastatic GIST. (Top right) CT image at same level demonstrates the 2 hypodense lesions in stomach and liver. (Bottom left) Transaxial bombesin image (SUV image) at level of CT image demonstrates clearly enhanced bombesin uptake only in liver lesion (SUV, 2.6). Bombesin uptake in stomach shows slight diffuse enhancement. (Bottom right) Fused image of ^{18}F -FDG and bombesin transaxial slice shows an agreement for both tracers in the liver lesion, whereas the enhanced ^{18}F -FDG uptake in the stomach is assigned to a low-bombesin-uptake area. Histology revealed recurrent stomach tumor and liver metastasis.

TABLE 1
Data Summary

Radiopharmaceutical	Parameter	Median	Mean	Minimum	Maximum
^{18}F -FDG	k1	0.544	0.580	0.199	0.961
	k2	0.803	0.780	0.500	0.999
	k3	0.092	0.107	0.003	0.314
	k4	0.003	0.006	0.000	0.023
	V_B	0.123	0.127	0.029	0.253
	Fractal dimension	1.376	1.351	1.158	1.440
	SUV	7.846	8.422	2.395	17.000
^{68}Ga -BZH ₃	k1	0.500	0.500	0.377	0.612
	k2	0.590	0.580	0.218	0.902
	k3	0.022	0.047	0.000	0.189
	k4	0.001	0.025	0.000	0.134
	V_B	0.188	0.231	0.050	0.588
	Fractal dimension	1.214	1.160	0.870	1.400
	SUV	3.270	3.270	0.536	9.253

for the tracer ^{68}Ga -DOTATOC, a substrate for somatostatin receptor subtype 2, which was applied in patients with meningiomas and neuroendocrine tumors at our institution using the same methodology (17,18). The reported mean k3 for DOTATOC in neuroendocrine tumors was 0.113, in comparison with 0.047 for bombesin in GIST, whereas the reported mean k1 for DOTATOC in neuroendocrine tumors was 0.529, in comparison with 0.5 for bombesin in GIST. The data may indicate a higher internalization rate for DOTATOC than for bombesin.

From the diagnostic point of view, the ^{18}F -FDG studies were superior and revealed enhanced uptake in 25 of 30 lesions. However, 2 lesions in the gastrointestinal tract were false-positive with ^{18}F -FDG, as subsequently shown by clinical follow-up data. Whether these false-positive results could have been avoided by using a combined PET/CT scanner is an open question. Interestingly, a histologically confirmed recurrent stomach tumor that could not be delineated on the ^{18}F -FDG study demonstrated enhanced ^{68}Ga -BZH₃ uptake (Fig. 1). It is reported that ^{18}F -FDG primarily measures viable tumor tissue (19). In contrast, it is also known that there is an association between ^{18}F -FDG uptake and proliferation rate (20). Therefore, a possible explanation for the low ^{18}F -FDG uptake may be the low viability or the low proliferative activity as measured by Ki-67 (<10%).

Generally, ^{68}Ga -BZH₃ uptake was lower than ^{18}F -FDG uptake, and only a subgroup (41%) of the patients demonstrated enhanced uptake. This finding differs from that in 15 patients with neuroendocrine tumors studied with ^{68}Ga -DOTATOC, all of whom demonstrated enhanced DOTATOC uptake (57/63 evaluated lesions) (18). The data differ from the present study, in which only 7 of 17 patients with GIST demonstrated enhanced ^{68}Ga -BZH₃ accumulation (mean SUV of 3.3, compared with the surrounding tissue). The data give evidence of a subgroup (41%) of GIST patients who demonstrate enhanced receptor expression. On the basis of these preliminary results, receptor scintigraphy with bombesin cannot be generally recommended. The idea of performing radionuclide therapy—analogueous to giving ^{90}Y -DOTATOC therapy to patients with neuroendocrine tumors—cannot be supported by these results because of the relatively low uptake in most patients. Further studies on larger numbers of patients are needed to confirm these results.

CONCLUSION

Quantitative ^{18}F -FDG data showed enhanced viability in 25 of 30 lesions (14/17 patients; median SUV, 7.9). Only 8 of 30 lesions (7/17 patients) demonstrated enhanced ^{68}Ga -BZH₃ uptake (median SUV, 3.3). One recurrent GIST in

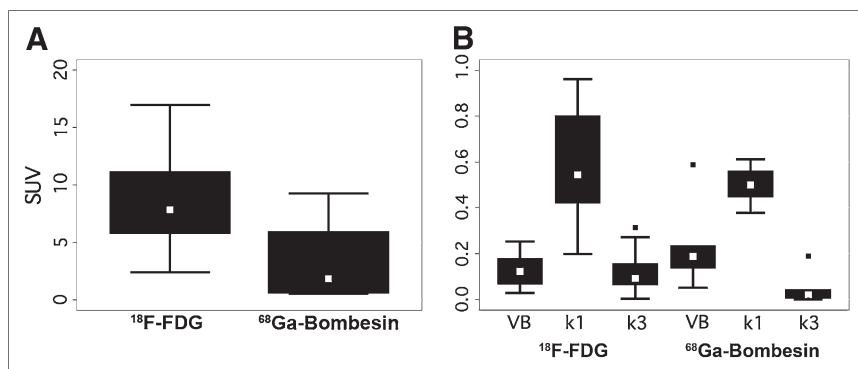


FIGURE 4. (A) Box-and-whisker plot of median SUV for both tracers 56–60 min after injection in malignant lesions. (B) Box-and-whisker plot of median values for both tracers for V_B , k1, and k3 in malignant lesions.

the stomach was delineated only on the $^{68}\text{Ga-BZH}_3$ scans; $^{18}\text{F-FDG}$ uptake was low. The data demonstrate a subgroup of GIST lesions that show enhanced bombesin receptor expression. The meaning of the enhanced $^{68}\text{Ga-BZH}_3$ uptake is not yet certain.

REFERENCES

1. Demetri GD, von Mehren M, Blanke CD, et al. Efficacy and safety of imatinib mesylate in advanced gastrointestinal stromal tumors. *N Engl J Med.* 2002;347:472–480.
2. Koukouraki S, Strauss LG, Georgoulis V, et al. Evaluation of the pharmacokinetics of $^{68}\text{Ga-DOTATOC}$ in patients with metastatic neuroendocrine tumors scheduled for $^{90}\text{Y-90-DOTATOC}$ therapy. *Eur J Nucl Med Mol Imaging.* 2005;33:460–466.
3. Reubi JC, Körner M, Waser B, Mazzucchelli L, Guillou L. High expression of peptide receptors as a novel target in gastrointestinal stromal tumours. *Eur J Nucl Med Mol Imaging.* 2004;31:803–810.
4. Schuhmacher J, Zhang H, Doll J, et al. GRP receptor-targeted PET of a rat pancreas carcinoma xenograft in nude mice with a ^{68}Ga -labeled bombesin (6-14) analog. *J Nucl Med.* 2005;46:691–699.
5. Toorongian SA, Mulholland GK, Jewett DM, Bachelor MA, Kilbourn MR. Routine production of 2-deoxy-2-(^{18}F)fluoro-D-glucose by direct nucleophilic exchange on a quaternary 4-aminopyridinium resin. *Int J Rad Appl Instrum B.* 1990;17:273–279.
6. Strauss LG, Conti PS. The applications of PET in clinical oncology. *J Nucl Med.* 1991;32:623–648.
7. Burger C, Buck A. Requirements and implementations of a flexible kinetic modeling tool. *J Nucl Med.* 1997;38:1818–1823.
8. Mikolajczyk K, Szabatin M, Rudnicki P, Grodzki M, Burger C. A Java environment for medical image data analysis: initial application for brain PET quantitation. *Med Inform (Lond).* 1998;23:207–214.
9. Miyazawa H, Osmont A, Petit-Taboue MC, et al. Determination of ^{18}F -fluoro-2-deoxy-D-glucose rate constants in the anesthetized baboon brain with dynamic positron tomography. *J Neurosci Methods.* 1993;50:263–272.
10. Sokoloff L, Smith CB. Basic principles underlying radioisotopic methods for assay of biochemical processes in vivo. In: Greitz T, Ingvar DH, Widén L, eds. *The Metabolism of the Human Brain Studied with Positron Emission Tomography.* New York, NY: Raven Press; 1983:123–148.
11. Ohtake T, Kosaka N, Watanabe T, et al. Noninvasive method to obtain input function for measuring glucose utilization of thoracic and abdominal organs. *J Nucl Med.* 1991;32:1432–1438.
12. Dimitrakopoulou-Strauss A, Strauss LG, Mikolajczyk K, et al. On the fractal nature of dynamic positron emission tomography (PET) studies. *World J Nucl Med.* 2003;2:306–313.
13. Stroobants S, Goeminne J, Seegers M, et al. ^{18}F -FDG-positron emission tomography for the early prediction of response in advanced soft tissue sarcoma treated with imatinib mesylate (Glivec). *Eur J Cancer.* 2003;39:2012–2020.
14. Goerres GW, Stupp R, Barghouth G, et al. The value of PET, CT and in-line PET/CT in patients with gastrointestinal stromal tumours: long-term outcome of treatment with imatinib mesylate. *Eur J Nucl Med Mol Imaging.* 2005;32:153–162.
15. Dimitrakopoulou-Strauss A, Georgoulis V, Eisenhut M, et al. Quantitative assessment of SSTR2 expression in patients with non-small cell lung cancer using $^{68}\text{Ga-DOTATOC}$ PET and comparison to $^{18}\text{F-FDG}$ PET. *Eur J Nucl Med Mol Imaging.* 2006;33:823–830.
16. Zhang X, Cai W, Cao F, et al. ^{18}F -Labeled bombesin analogs for targeting GRP receptor-expressing prostate cancer. *J Nucl Med.* 2006;47:492–501.
17. Henze M, Dimitrakopoulou-Strauss A, Milker-Zabel S, et al. Characterization of $^{68}\text{Ga-DOTA-D-PHE1-TYR3-octreotide}$ kinetics in patients with meningiomas. *J Nucl Med.* 2005;46:763–769.
18. Koukouraki S, Strauss LG, Georgoulis V, et al. Comparison of pharmacokinetics of $^{68}\text{Ga-DOTATOC}$ and $^{18}\text{F-FDG}$ in patients with metastatic neuroendocrine tumours scheduled for $^{90}\text{Y-DOTATOC}$ therapy. *Eur J Nucl Med Mol Imaging.* 2006;33:1115–1122.
19. Higashi K, Clavo AC, Wahl RL. Does FDG uptake measure proliferative activity of human cancer cells? In vitro comparison with DNA flow cytometry and tritiated thymidine uptake. *J Nucl Med.* 1993;34:414–429.
20. Strauss LG, Dimitrakopoulou-Strauss A, Koczan D, et al. $^{18}\text{F-FDG}$ kinetics and gene expression in giant cell tumors. *J Nucl Med.* 2004;45:1528–1535.